Fracture detection (AVAZ): ambiguity and practical solution

Ye Zheng[1], Dragana Todorovic-Marinic[1] and Glenn Larson[2]
[1]Veritas DGC, Calgary, Alberta, Canada, [2]Devon Canada Corp., Calgary, Alberta, Canada

2004 CSEG National Convention

Summary

It is becoming popular to extract fracture information from wide-azimuth P-P reflection seismic data. The extracted fracture density is little influenced by the phase of the seismic data. The extracted fracture orientation is sensitive to the phase of seismic data and the types of geological interfaces. Other information besides the amplitude of seismic data is needed in order to uniquely determine the fracture orientation. This paper discusses the ambiguity of the fracture orientation and how it can be resolved. Todorovic-Marinic et al (2004) discuss the stabilization of fracture density.

Introduction

Extracting fracture information from P-P reflection seismic data recently became a hot topic (Gray et al, 1999, 2000, Hall et al, 2000, Li, 1999, Lynn et al, 1996, MacBeth and Lynn, 2001). A fractured reservoir can be considered as an azimuthal anisotropic medium (or horizontally transverse isotropic medium). P and S wave velocities vary with the azimuth of the incident ray path. The amplitude of reflected P waves vary with azimuth as well (Thomsen, 1988). From the variation of the amplitude at different azimuths, one can extract fracture density and orientation (Lynn et al, 1996). Practically, fracture density extracted from seismic data is relatively stable. However, the extracted fracture orientation is sensitive to the phase of the seismic data and the types of geological interfaces.

The amplitude of reflected P wave on the interface between two azimuthal anisotropic media varies at different incident angles and azimuths of the ray path. The variation can be described as (Rüger, 2002):

$$R(\theta,\varphi) = A + [B^{iso} + B^{ani}\cos^2(\varphi - \varphi_{sym})]\sin^2\theta \qquad (1)$$

where *R* is the reflectivity (amplitude) of the P wave. A is the AVO intercept. B^{iso} is the isotropic AVO gradient. B^{ani} is the fracture density (anisotropic gradient). θ is the incident angle of the seismic wave, φ is the azimuth of the ray path, and φ_{sym} is the azimuth of the direction perpendicular to the fracture strike. For a given offset (or incident angle), the amplitude variation curve is a sinusoid with a period of 180 degrees. There are four unknowns in the equation, A, B^{iso}, B^{ani} and $\varphi_{sym.}$ Note that mathematically we can never get the unique solution from equation (1) no matter how much data are available. If we change the sign of B^{ani}, regroup B^{iso} and at the same time rotated φ_{sym} by 90 degrees, we can get another set of B^{iso}, B^{ani} and φ_{sym} that still satisfy the equation. One might force B^{ani} to be positive, but now the detected fracture orientation is questionable, because at the real world, B^{ani} could be positive or negative.

The above discussion is based on zero phase data and did not consider side lobes. When we deal with a seismic dataset with arbitrary phase and take the side lobes into account, things become more complicated.

Synthetic tests

Synthetic datasets are created to test the fracture detection result with different phases of seismic data. The synthetic datasets are modeled using equation (1). This will give us some idea how the phase of the seismic data affects the results of fracture detection. The model has two layers, an isotropic layer on top of an anisotropic layer. A synthetic gather with a zero phase Ricker wavelet is created using equation (1). Then the gather is phase rotated by 30 degrees to create a series of gathers with different phases. Fracture detection is then applied to these gathers. In the inversion, B^{ani} is forced to be positive. Figure 1 shows the model and the results of fracture detection for different phases. Panel 8, on the far right side, is the model used for the test. The reflection interface is a Class I type interface (Rutherford & Williams, 1989) with positive intercept (A) and negative gradient (B^{iso}). The fracture orientation is set to 45 degrees (φ_{sym}) and the fracture density (B^{ani}) is positive. The second panel from the right side (panel 7) is the result of fracture detection from the zero phase gather. On the far left side, panel 1, is the result of fracture detection from the 180 degrees phase-rotated (reversed polarity) gather. By comparing panels 1 and 7, one can notice that the detected fracture density is the same, but the fracture orientation is rotated by 90 degrees for each time sample. For the phase of the gather between 0 and 180 degrees, the detected fracture orientation is the same for some time samples and is rotated by 90 degrees for other samples. Looking at all panels from 1 – 7, one finds that the detected fracture orientation is rotated by 90 degrees wherever the intercept is negative. The average fracture density over a wavelength remains same for the gathers rotated with different phases.

Now let's take a look at another synthetic example. A Class III type of interface is modeled. The same procedure was used as previous example. The results are shown in Figure 2. Similar to the previous case, when the phase of the input gather is rotated by 180 degrees, the detected fracture orientation is rotated by 90 degrees. And the average fracture density over a wavelength is the same for all gathers. However, in this case, the correct fracture orientation is detected when the intercept is negative.

Other classes were tested using the same procedures as described above. From the results of the tests, one can find that the detected fracture density is independent of the phase of the seismic gathers in terms of the average over a wavelet length. The detected fracture orientation rotates 90 degrees when the AVO intercept changes polarity. And there is no specific tie between the polarity of AVO intercept and the correct fracture orientation.

Field data example

Copton 3D seismic dataset from the Narraway gas field in Alberta is used to test the impact of different phases of the seismic gathers on the detected fracture orientation. Fracture detection is applied to an area of 9 X 17 CMPs. The CMP bin size is 35 X 70 m^2. The test area is about 630 X 595 m^2. Figure 3 shows a stacked line in the middle of the test area (left) and three time slices of detected fracture density and orientation (right). There is a short line in each CMP bin. The length of the bar represents the detected fracture density and the direction of the bar represents the fracture orientation. The polarity of the stacked traces is negative for most CMPs at 1792 ms and positive at 1800 ms. The detected fracture orientations at 1792 ms are perpendicular to the fracture orientations at 1800 ms for most CMP bins. Since the data are from a structured area and seismic traces from a group of CMPs are used for fracture detection, the detected fracture orientation may not just rotate by 90 degrees when the polarity changes as in the synthetic data. At 1796 ms, some traces are on the positive side and some on negative side. Therefore the detected fracture orientations are close to what at the previous time sample (1792 ms) for some CMPs and the nest time sample (1800 ms) for others.

In order to solve the ambiguity of the detected fracture orientation, geological interpretation and well logging data were integrated. In Figure 4, the top (red) and bottom (purple) of the reservoir, the Fahler G formation, are marked at the location of well 11-24. The detected fracture orientation at the top is -40^{o} and at the bottom, 50^{o}. FMI log indicates that the fracture orientation in the Fahler G formation is 55^{o}. Therefore the orientation detected from seismic data is correct at the bottom and off at the top of the reservoir. The information from the interpretation of the FMI log solves the ambiguity. The contrast of fracture density shows there are fracture density changes at the top and bottom of the reservoir. The envelope method (Todorovic-Marinic et al 2003) gives better image of fracture density.

Conclusions

The inversion result from equation (1) is not unique. If the fracture density (B^{ani}) is forced to be positive, the fracture orientation from the inversion is sensitive to the phase of seismic data and the types of geological interfaces. The detected fracture orientation rotates 90 degrees when the AVO intercept polarity changes. There is no specific tie between the polarity of AVO intercept and the correct fracture orientation. The addition of information besides the seismic amplitudes is required to resolve the ambiguity in the fracture orientation. In the case shown here, the FMI log helps solve the ambiguity of the detected fracture orientation. The detected fracture density is stable and independent of the phase of input data in terms of the average value over a wavelength.

Acknowledgements

The authors had very helpful discussions with David Gray and would like to take this opportunity to thank him for his help.

References

Gray, F.D., Head, K.J., Chamberlain, C.K., Olson, G., Sinclair, J. and Besler, C., 1999, Using 3D Seismic to Identify Spatially Variant Fracture Orientation in the Manderson Field: SPE Paper 55636.

Gray, F.D. and Head, K.J., 2000, Fracture Detection in the Manderson Field: A 3D AVAZ Case History: The Leading Edge, Vol. 19, No. 11, 1214-1221.

Hall, S., Kendall, J.M., Barkved, O. and Mueller, M., 2000, Fracture characterization using P-wave AVOA in 3-D OBS data: 70th Ann. Internat. Mtg: Soc. Of Expl. Geophys., 1409-1412.

Li, X. -Y., 1999, Fracture detection using azimuthal variation of P-wave moveout from orthogonal seismic survey lines: Geophysics, Soc. of Expl. Geophys., **64,** 1193-1201.

Lynn, H.B., Simon, K.M. and Bates, C.R., 1996, Correlation between P-wave AVOA and S-wave traveltime anisotropy in a naturally fractured gas reservoir: The Leading Edge, 15, 8, 931-935.

MacBeth, C. and Lynn, H., 2001, Mapping fractures and stress using full-offset full-azimuth 3D PP data: 71st Ann. Internat. Mtg: Soc. of Expl. Geophys., 110-113.

Rüger, A., 2002, Reflection Coefficients and Azimuthal AVO Analysis in Anisotropic Media: Geophysical Monograph Series, Number 10, Soc. of Expl. Geophys.

Rutherford, S.R. and Williams, R.H., 1989, Amplitude-versus-offset variations in gas sands: Geophysics, 54, 680-688.

Thomsen, L., 1988, Reflection seismology over azimuthally anisotropic media: Geophysics, 53, 304-313.

Todorovic-Marinic, D., Gray, F.D., Zheng, Y., Larson, G. and Pelletier, J., 2003, Envelope of Fracture Density: Presented at the Joint CSEG/CSPG Convention.

Todorovic-Marinic, D., Larson, G., Gray, D., Soule, G., Zheng, Y. and Pelletier, J. 2004, Identifying vertical productive fractures in the Narraway gas field using the envelope of seismic anisotropy: submitted for CSEG convention.

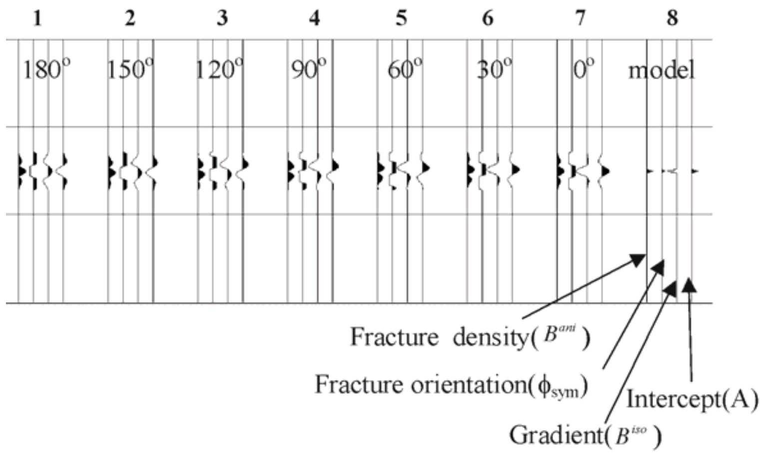

Figure 1. A Class I model (panel 8) is used to test the fracture detection result with different phases of seismic data. The model gather (not shown) is rotated by different amounts. The results of fracture detection for each rotation are shown in panels 1 – 7. The detected fracture orientation is correct when the AVO intercept is positive.

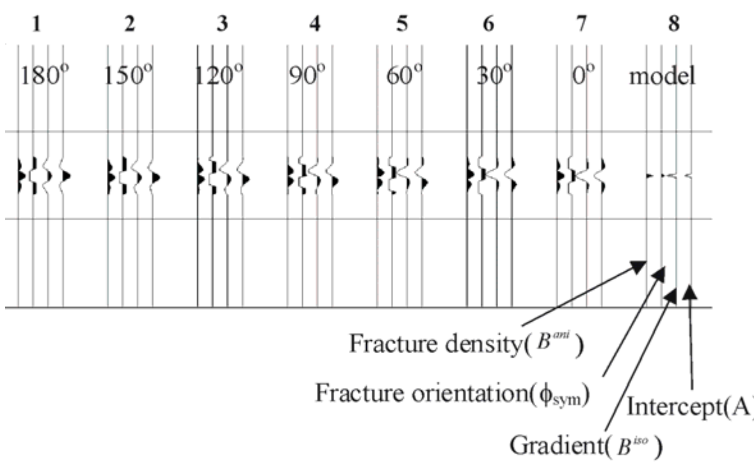

Figure 2. A Class III model (panel 8) is used to test the fracture detection result with different phases of seismic data. The model gather (not shown) is rotated by different amounts. The results of fracture detection for each rotation are shown in panels 1 – 7. The detected fracture orientation is correct when AVO intercept is negative.

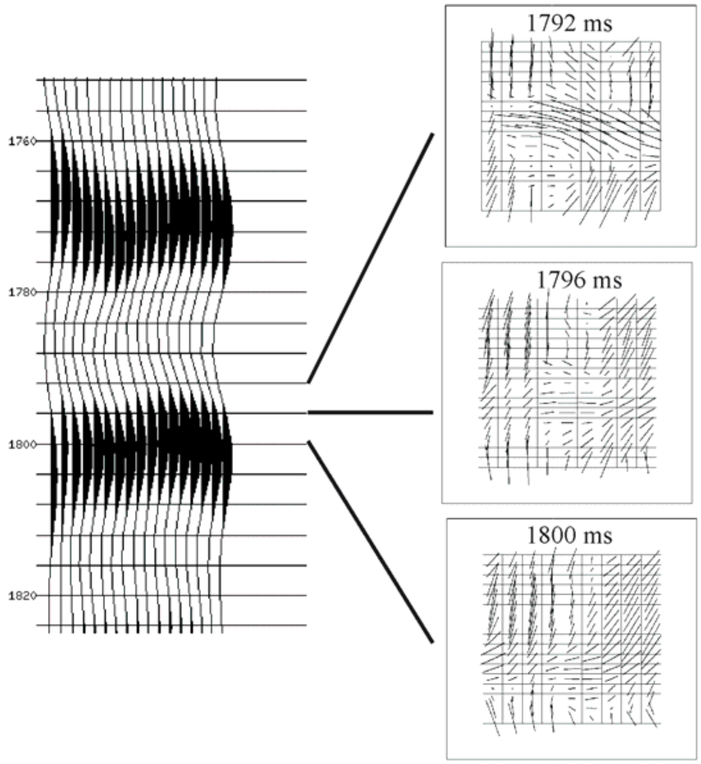

Figure 3. Three adjacent time slices of fracture density and orientation detected from a seismic dataset in Alberta, Canada are shown on the right side. The length of the short lines in every CMP bin represents the fracture density and the direction of the lines represents the fracture orientation. On the left side, it is a line of stacked section (in the middle of the test area). The detected fracture orientation rotates 90^{o} when the polarity of the stacked section changes.

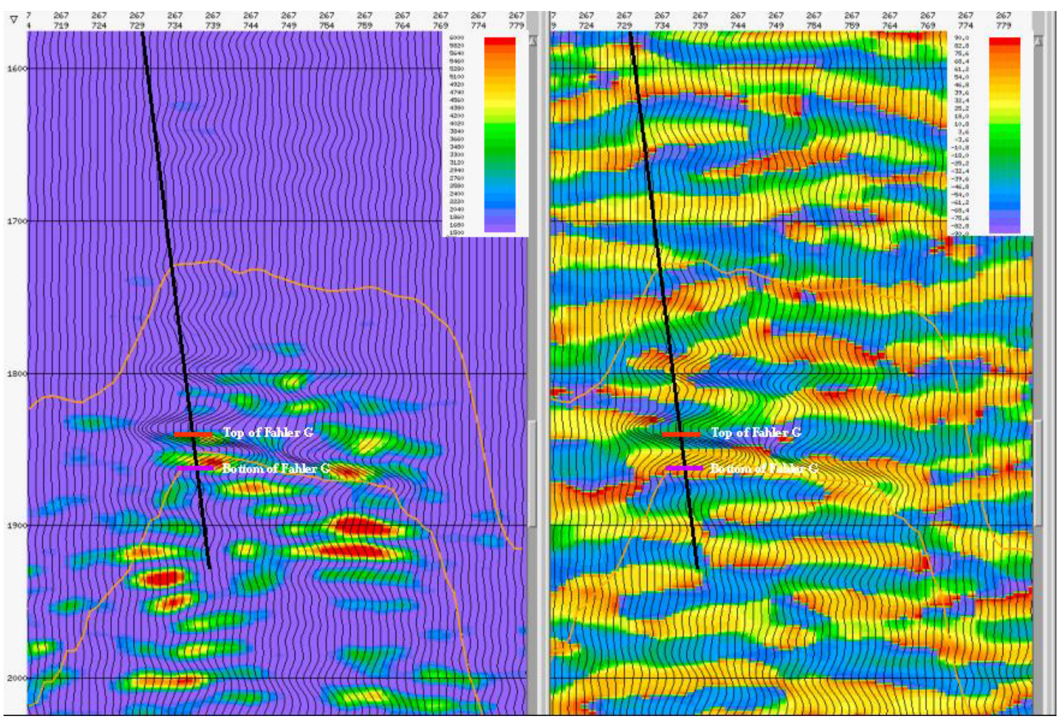

Figure 4. The left panel is P wave reflectivity (wiggle) overlaid by fracture density contrast (color). The right panel is P wave reflectivity (wiggle) overlaid by fracture orientation (color). The top (red) and bottom (purple) of the reservoir (Fahler G) is marked on the well 11-24 (black tilted line). At the bottom of the reservoir, AVAZ gives correct fracture orientation. However, at the top of the reservoir, the orientation is 90^{o} off.